



# An Environmental Model of Honey Bee Colony Collapse Due to Pesticide Contamination

P. Magal<sup>1</sup> · G. F. Webb<sup>2</sup> · Yixiang Wu<sup>2</sup>

Received: 30 May 2019 / Accepted: 4 September 2019  
© Society for Mathematical Biology 2019

## Abstract

We develop a model of honey bee colony collapse based on the contamination of forager bees in environmental regions contaminated with pesticides. An important feature of the model is the daily homing capacity each day of foragers bees. The model consists of difference equations describing the daily homing of uncontaminated and contaminated forager bees, with an increased homing failure of contaminated bees. The model quantifies colony collapse in terms of the fraction of contaminated bees subject to this increased homing failure. If the fraction is sufficiently high, then the hive falls below a viability threshold population size that leads to rapid disintegration. If the fraction is sufficiently low, then the hive can rise above the viability threshold and attain a stable population level.

**Keywords** Colony collapse · Pesticide contamination · Difference equation

**Mathematics Subject Classification** 92D25 · 92D40

## 1 Introduction

Our objective is to analyze the role of pesticide contamination in honey bee colony collapse disorder (CCD). CCD is defined as the disappearance of a majority of honey bees in a colony, leaving behind insufficient numbers of bees to care for immature bees in the hive (Myerscough et al. 2017; Wikipedia 2019). CCD occurs in both

---

✉ G. F. Webb  
glenn.f.webb@vanderbilt.edu

P. Magal  
pierre.magal@u-bordeaux.fr

Yixiang Wu  
yixiang.wu@mtsu.edu

<sup>1</sup> Université de Bordeaux, Bordeaux, France

<sup>2</sup> Vanderbilt University, Nashville, TN, USA

natural wild settings and in managed agricultural settings. CCD losses in managed honey bee colonies have increased markedly worldwide and in the USA in recent years (Bee Informed Partnership 2018; Goulson et al. 2015; United States Department of Agriculture Agricultural Research Service 2019). Various causes of CCD have been proposed, including viral infection transmitted by mites and environmental contamination arising from fungicides and pesticides. Mathematical models of CCD caused by viral infections include Becher et al. 2014; Bernardi and Venturino 2016; Betti et al. 2014; DeGrandi-Hoffman and Curry 2004; Farley 2017; Kang et al. 2016; Khoury et al. 2011; Martin 2002; Ratti et al. 2013, 2015, 2017; Russell et al. 2013; Sumpter and Martin 2004. Mathematical models of CCD caused by environmental contamination arising from fungicides and pesticides include Becher et al. 2014; Betti et al. 2014, 2017; Henry et al. 2012, 2015; Schmickl and Crailsheim 2007; Willkinson and Smith 2002. Surveys of mathematical models for CCD are given in Becher et al. (2013, 2018).

The significance of environmental pesticide contamination (EPC) in CCD is controversial, since it is recognized that pesticides have sub-lethal effects on honey bees, but may cause delayed development and impaired functionality of forager bees that become contaminated (Barron 2015; Blacqui re et al. 2016; Bryden et al. 2013; Henry et al. 2012, 2015; Kang and Theraulaz 2016; Khoury et al. 2011; Meikle et al. 2016; Sandrock et al. 2014). Forager bees differentiate from hive worker bees at approximate age of 21 days, at which time they transition to performing out-colony tasks, including water, nectar, pollen, and resin collection (Abou-Shaara 2014). The contribution of forager bees to the rearing of juvenile bees in the hive is significant and is regulated by the number of forager bees in the colony, a process known as social inhibition (Betti et al. 2014; Huang and Robinson 1974; Leoncini et al. 2004).

A class of neuro-active insecticides, neonicotinoids, have been identified as potentially harmful to honey bee colonies, particularly to managed colonies, whose foragers have exposure to contaminated agricultural fields (Blacqui re et al. 2016; Chauzat et al. 2009; Desneux et al. 2007; Thompson et al. 2015). In Europe, neonicotinoid pesticide products have been partially banned in agricultural use (European Food Safety Authority 2018). In the USA, neonicotinoids have been banned in some states (American Society for Horticultural Science 2019), and legislation is pending in the US Congress for a national ban (United States Environmental Protection Agency 2019; H.R. 3040-Saving America's Pollinators Act 2018). A recent study by the European Food Safety Authority has confirmed the risk of neonicotinoids to bees (European Food Safety Authority 2018b). Another study by the Genetic Literacy Project has disputed this claim, citing studies that found limited linkage of CCD to neonicotinoid contamination (Cutler and Scott-Dupree 2007; Cutler et al. 2014; Cutler and Scott-Dupree 2016; Dively et al. 2015; Nguyen et al. 2009; Pilling et al. 2013; Rolke et al. 2016; Rundlof et al. 2015; Schneider et al. 2012; Stanley et al. 2016).

Recent studies by Henry et al. (2012, 2015) have identified neonicotinoid pesticides as responsible for significant homing failure in forager honey bees. In these studies, free-ranging individual forager bees were monitored with radio-frequency identification. In one field study, a fraction 0.2–0.3 of exposed foragers failed to return to their colony on a daily basis, when foraging in treated crop regions, which was as much as twice the fraction of homing failure of unexposed foragers. Forager bees, when they

return each day from foraging, provide a significant contribution for brood rearing in the hive (DeGrandi-Hoffman et al. 1989). Thus, increased homing failure may significantly destabilize the social organization in the development of new bees in the colony population, resulting in CCD.

In this paper, we analyze a model of CCD arising from pesticide contamination. Our model has the form of a discrete-time difference equation, which tracks forager bees as they leave and return to the hive each day. This daily homing feature is of major importance in understanding the consequences of pesticide contamination upon homing capacity. Our modeling approach here is applicable to many biological species that exhibit such a regular return-home behavior. In the future work, we will analyze a spatially dependent version of the model here.

Our model of EPC describes only the forager bees in the colony, since worker bees, drone bees, and the queen bee are not contaminated directly. Our model describes the forager population day by day, and our time unit will be a day, defined as the period of sunlight during each day. We note that this sunlight period may vary from one location to another. Our model is designed for shorter time spans, typical of managed colonies placed in agricultural fields, rather than for seasonal time spans characteristic of natural colonies in the wild, in which colony size varies considerably throughout the year.

A key element of our analysis is a critical viable threshold of the forager bee population (Dennis and Kemp 2016; Myerscough et al. 2017). If the population falls below this threshold, CCD will rapidly occur. If the population is above this threshold, the colony can stabilize. This population behavior is often called an *Allee effect*, which can have a variety of modeling forms. Allee effects have been used in many models of CCD, in both gain and loss terms (Banks et al. 2017; Bernardi and Venturino 2016; Betti et al. 2014; Booten et al. 2017; Bryden et al. 2013; Dennis and Kemp 2016; Gabbriellini 2017; Goulson et al. 2015; Kang and Theraulaz 2016; Kang et al. 2016; Kribs-Zaleta and Mitchell 2014; Myerscough et al. 2017; vanEngelsdorp et al. 2009). In our model, the Allee effect will be placed in the term corresponding to the production of new forager bees, as they transition from eclosion, maturation, and differentiation to forager functionality.

The organization of this paper is as follows: in Sect. 2 we develop a model of CCD without pesticide contamination; in Sect. 3 we develop a model of CCD with pesticide contamination based on the homing failure fraction of contaminated foragers; in Sect. 4 we illustrate the model with numerical simulations; in Sect. 5 we provide some conclusions from our model of EPC in CCD.

## 2 Model Without Pesticide Contamination

We first consider a honey bee colony without exposure to pesticide contamination. At sunrise of the first day, the number of forager bees is

$$U(0) = U_0 \geq 0.$$

During the first day, the population of bees is subject to natural loss, which includes homing failure, and all other causes of mortality. The change in  $U(t)$  during the first day is described by the following differential equation:

$$U'(t) = -\mu U(t), t \in [0, 1),$$

where  $\mu > 0$  is the natural mortality rate of forager bees, including homing failure. The units of  $\mu$  are  $\text{day}^{-1}$ , and the number of forager bees who survived to the end of the first day is denoted by

$$U(1^-) = e^{-\mu}U_0,$$

where  $\mu$  is multiplied by 1 day.

At sunrise of the second day, we account for the recruitment of new hive bees to foraging. This maturation process of hive bees requires up to 3 weeks, from eclosion to adulthood specialization to foraging. We set the number of new forager bees at the beginning of the second day to

$$\frac{\beta U(1^-)^2}{\chi^2 + U(1^-)^2}.$$

This Allee form term for forager recruitment means that when the number of forager bees is below a viability threshold, the production of new forager bees decreases sharply, and when the number of forager bees is large, the number of recruited forager bees approaches  $\beta$ , which is the maximal rate of new forager bees produced per day. This form for recruitment of new forager bees emphasizes the role of forager bees, in addition to hive worker bees, in the rearing of hive bees.

Thus, the number of new forager bees at the beginning of the second day is

$$\begin{aligned} U_1 &= \frac{\beta U(1^-)^2}{\chi^2 + U(1^-)^2} + U(1^-) \\ &= \frac{\beta U(0)^2}{\tilde{\chi}^2 + U(0)^2} + e^{-\mu}U(0) \end{aligned}$$

where  $\tilde{\chi} = \chi e^\mu$ . Therefore, we obtain the following difference equation to describe the number of forager bees at sunrise of day  $n + 1$ :

$$\begin{cases} U(n + 1) = \frac{\beta U(n)^2}{\tilde{\chi}^2 + U(n)^2} + e^{-\mu}U(n), & n \geq 0, \\ U(0) = U_0, \end{cases} \tag{1}$$

The number of bees during day  $n = 0, 1, \dots$  is

$$U(t) = e^{-\mu(t-n)}U(n), t \in [n, n + 1).$$

**Equilibria:** 0 is always an equilibrium of (1). A strictly positive equilibrium  $\bar{U}$  of 1 must satisfy the following equality:

$$\frac{\tilde{\beta}\bar{U}}{\tilde{\chi}^2 + \bar{U}^2} = 1$$

where

$$\tilde{\beta} := \frac{\beta}{(1 - e^{-\mu})}.$$

Therefore, we seek the positive roots of

$$p(U) = U^2 - \tilde{\beta}U + \tilde{\chi}^2 = 0.$$

Set

$$R_0 := \frac{\tilde{\beta}}{2\tilde{\chi}} = \frac{\beta e^{-\mu}}{2\chi(1 - e^{-\mu})}.$$

We observe that if  $R_0 < 1$ ,  $p(U)$  has no real root, and if  $R_0 > 1$ ,  $p(U)$  has two positive roots.

Since the right-hand side of the difference equation (1) is monotone, we obtain the following result:

**Lemma 1** (Allee effect) *We have the following alternatives:*

- (i) *If  $R_0 < 1$ , the only equilibrium of (1) is 0. Moreover, 0 is stable for (1) and every solution starting from  $U_0 \geq 0$  converges to 0.*
- (ii) *If  $R_0 > 1$ , (1) has three nonnegative equilibria:*

$$0 < \bar{U}_- := \frac{\tilde{\beta} - \sqrt{\tilde{\beta}^2 - 4\tilde{\chi}^2}}{2} < \bar{U}_+ := \frac{\tilde{\beta} + \sqrt{\tilde{\beta}^2 - 4\tilde{\chi}^2}}{2}.$$

*Moreover, 0 is locally stable for (1) and every solution of (1) starting from  $U_0 \in [0, \bar{U}_-)$  converges to 0. Furthermore,  $\bar{U}_+$  is locally stable and every solution of (1) starting from  $U_0 \in (\bar{U}_-, \infty)$  converges to  $\bar{U}_+$ .*

**Proof** Define

$$f(x) = \frac{\beta x^2}{\tilde{\chi}^2 + x^2} + e^{-\mu}x,$$

which corresponds to the right-hand side of (1).

*Proof of (i):* Assume  $R_0 < 1$ . Then  $f(x) < x$  for all  $x > 0$ , and

$$U(1) = f(U(0)) < U_0.$$

Since  $f(x)$  is strictly increasing, by applying  $f$  on both sides of the above inequality  $n$  times, we deduce that

$$U(n + 1) = f^n(U(1)) < f^n(U(0)) = U(n).$$

Therefore,  $n \rightarrow U(n)$  is decreasing. Since this sequence is bounded, it converges to the largest equilibrium below  $U(0)$  which is 0. Therefore,  $U(n)$  converges to 0 as  $n \rightarrow \infty$ .

*Proof of (ii):* Assume  $R_0 > 1$ . If  $U(0) \in (0, \bar{U}_-)$ , then

$$U(1) = f(U(0)) < U_0,$$

and by using the same argument as above,  $U(n)$  converges to 0 as  $n \rightarrow \infty$ . If  $U(0) \in (\bar{U}_-, \bar{U}_+)$ , then

$$U(1) = f(U(0)) > U_0$$

and by using the same argument as above,  $U(n)$  converges to  $\bar{U}_+$  which is the smallest equilibrium above  $U(0)$ . Similarly, when  $U(0) > \bar{U}_+$ , we have

$$U(1) = f(U(0)) < U_0$$

and by using the same argument as above,  $U(n)$  converges to  $\bar{U}_+$ , which is the largest equilibrium below  $U(0)$ . □

**Identification of the parameters:** In a particular application,  $\bar{U}_+$  and  $\bar{U}_-$  may be known. We set

$$\frac{\tilde{\beta} + \sqrt{\tilde{\beta}^2 - 4\tilde{\chi}^2}}{2} = \bar{U}_+ \tag{2}$$

and

$$\frac{\tilde{\beta} - \sqrt{\tilde{\beta}^2 - 4\tilde{\chi}^2}}{2} = \bar{U}_-. \tag{3}$$

By summing (2) and (3), we obtain

$$\tilde{\beta} = \bar{U}_+ + \bar{U}_- = \frac{\beta}{1 - e^{-\mu}}, \tag{4}$$

and subtracting (3) from (2), we obtain

$$\tilde{\chi}^2 = \frac{(\bar{U}_+ + \bar{U}_-)^2 - (\bar{U}_+ - \bar{U}_-)^2}{4} = \chi^2 e^{2\mu}. \tag{5}$$

Therefore, if  $\mu$ ,  $\bar{U}_-$ , and  $\bar{U}_+$  are known, we can identify the parameters  $\beta$  and  $\chi$  by using (4) and (5). An example is given in Fig. 1.

### 3 Model with Pesticide Contamination

In this section, we assume that the forager bees may be contaminated due to pesticide in the environment. At the sunrise of the first day, the numbers of uncontaminated and contaminated forager bees are

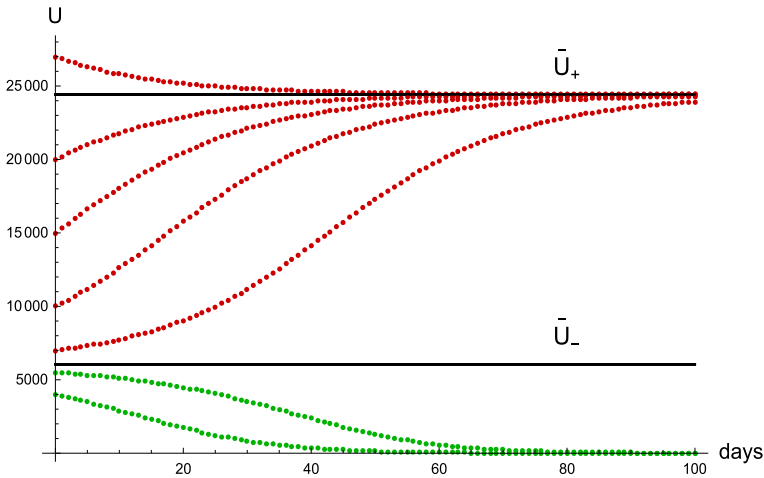


**Fig. 1** The values of the equilibria are  $\bar{U}_- = 6051$  and  $\bar{U}_+ = 24,423$ . The parameters are  $\beta = 2900$ ,  $\chi = 11,000$ ,  $\mu = 0.1$ .  $R_0 = 1.2534$ . The dots correspond to daily values (Color figure online)

$$U(0) = U_0 \geq 0, \quad C(0) = C_0 \geq 0.$$

During the day, the population of forager bees is subject to the natural mortality and contamination by pesticide in the environment. Thus, for  $t \in [0, 1)$ , we have

$$\begin{cases} U'(t) = -\mu U(t) - \alpha U(t) \\ C'(t) = -\mu C(t) + \alpha U(t) \end{cases} \tag{6}$$

where  $\alpha > 0$  is the rate of contamination during the day. A simple computation yields the populations at the end of the first day:

$$U(1^-) + C(1^-) = e^{-\mu}(U_0 + C_0), \quad U(1^-) = e^{-(\mu+\alpha)}U_0,$$

where  $\mu + \alpha$  is multiplied by one day. Therefore,

$$U(1^-) = e^{-(\mu+\alpha)}U_0, \quad C(1^-) = e^{-\mu} \{C_0 + [1 - e^{-\alpha}]U_0\}.$$

According to field experiments in Henry et al. (2012, 2015), the homing failure probability of forager bees, when foraging in treated contaminated crops on a daily basis, increased significantly, when compared to the natural homing failure of an uncontaminated forager. We thus obtain the following equations for the populations at the beginning of the second day:

$$\begin{cases} U_1 = \frac{\beta(U(1^-)+pC(1^-))^2}{\chi^2+(U(1^-)+pC(1^-))^2} + U(1^-), \\ C_1 = pC(1^-), \end{cases} \tag{7}$$

where  $p \in [0, 1]$  is the fraction of contaminated forager bees that succeeded in returning back to the hive at the end the first day. Thus,  $1 - p$  is the fraction of newly contaminated forager bees that have an increased mortality due to homing failure beyond the normal daily homing failure.

We start over at sunrise of the second day with the new initial conditions

$$U(1) = U_1, \quad C(1) = C_1.$$

We define

$$\begin{aligned} V(0) &:= U(1^-) + pC(1^-) = e^{-(\mu+\alpha)}U_0 + p(e^{-\mu}C_0 + [e^{-\mu} - e^{-(\alpha+\mu)}]U_0) \\ &= pe^{-\mu}(U_0 + C_0) + (1 - p)e^{-(\alpha+\mu)}U_0, \end{aligned}$$

which is the total population of forager bees that return to the hive at the end of the first day. Therefore, we obtain the following difference equation model that provides the numbers of uncontaminated and contaminated forager bees at sunrise of day  $n$ :

$$\begin{cases} U(n + 1) = \frac{\beta V(n)^2}{\chi^2 + V(n)^2} + e^{-(\mu+\alpha)}U(n), \\ C(n + 1) = pe^{-\mu}C(n) + pe^{-\mu}[1 - e^{-\alpha}]U(n), \end{cases} \tag{8}$$

where

$$V(n) := pe^{-\mu}C(n) + [pe^{-\mu} + (1 - p)e^{-(\alpha+\mu)}]U(n),$$

with initial condition

$$U(0) = U_0 \geq 0, \quad C(0) = C_0 \geq 0.$$

The terms in (8) have the following biological meaning:

$$\begin{cases} U(n + 1) = F(U(n), C(n)) \\ C(n + 1) = G(U(n), C(n)) \end{cases} \tag{9}$$

where

$$\underbrace{F(U, C)}_{\text{daily change in U}} = \underbrace{\frac{\beta V(U, C)^2}{\chi^2 + V(U, C)^2}}_{\text{daily production of new uncontaminated foragers U}} + \underbrace{e^{-\mu}e^{-\alpha}U}_{\text{daily survival and return home of uncontaminated foragers U}} \tag{10}$$

$$\underbrace{G(U, C)}_{\text{daily change in C}} = \underbrace{pe^{-\mu}C}_{\text{daily survival and return home of existing contaminated foragers C}} + \underbrace{pe^{-\mu}(1 - e^{-\alpha})U}_{\text{daily new C from contamination of U that survive and return home}} \tag{11}$$



$$\underbrace{V(U, C)}_{\substack{\text{daily total U and C} \\ \text{returning home}}} = \underbrace{pe^{-\mu}C}_{\substack{\text{daily survival} \\ \text{and return home} \\ \text{of existing C}}} + \underbrace{pe^{-\mu}(1 - e^{-\alpha})U}_{\substack{\text{daily new C that} \\ \text{survive and return home}}} + \underbrace{e^{-\mu}e^{-\alpha}U}_{\substack{\text{daily survival and} \\ \text{return home of} \\ \text{non-contaminated U}}} \quad (12)$$

### 3.1 Analysis of the Model with Contamination

We first consider the equilibria of the difference equation model (8).

**Equilibria:** (0, 0) is an equilibrium (8). By the second equation of (8), an equilibrium  $(\bar{U}, \bar{C})$  must satisfy the following equation

$$\bar{C} = pe^{-\mu} \{ \bar{C} + [1 - e^{-\alpha}] \bar{U} \} \Leftrightarrow \bar{C} = \kappa_1 \bar{U}$$

with

$$\kappa_1 := \frac{pe^{-\mu} [1 - e^{-\alpha}]}{1 - pe^{-\mu}}.$$

Moreover,

$$\bar{V} := e^{-\mu} \{ \bar{C} + [1 - e^{-\alpha}] \bar{U} \} = \kappa_2 e^{-(\mu+\alpha)} \bar{U}$$

where

$$\kappa_2 = e^{\alpha} \{ \kappa_1 + [1 - e^{-\alpha}] \} = \frac{e^{\alpha} - 1}{1 - pe^{-\mu}}.$$

Thus, the first equation of (8) gives

$$\bar{U} = \beta \frac{(e^{-(\mu+\alpha)} \bar{U} + p\kappa_2 e^{-(\mu+\alpha)} \bar{U})^2}{\chi^2 + (e^{-(\mu+\alpha)} \bar{U} + p\kappa_2 e^{-(\mu+\alpha)} \bar{U})^2} + e^{-(\mu+\alpha)} \bar{U}.$$

Thus, we obtain

$$\bar{U} = \frac{\hat{\beta} \bar{U}^2}{\hat{\chi}^2 + \bar{U}^2} \quad (13)$$

where

$$\hat{\beta} := \frac{\beta}{1 - e^{-(\mu+\alpha)}} \text{ and } \hat{\chi} := \frac{\chi}{e^{-(\mu+\alpha)} [1 + p\kappa_2]}. \quad (14)$$

By using the argument employed in Lemma 1, we derive the following quantity:

$$R_1 := \frac{\hat{\beta}}{2\hat{\chi}} = \frac{\beta [1 + p\kappa_2]}{2\chi [e^{(\mu+\alpha)} - 1]} = \frac{\beta [[1 - pe^{-\mu}] + p[e^{\alpha} - 1]]}{2\chi [e^{(\mu+\alpha)} - 1] [1 - pe^{-\mu}]},$$

We thus obtain

**Lemma 2** *The following alternatives holds:*

- (i) *If  $R_1 < 1$ , then  $(0, 0)$  is the only equilibrium of system (8).*
- (ii) *If  $R_1 > 1$ , then system (8) has three equilibria:*

$$(0, 0) \ll (\bar{U}_-, \bar{C}_-) \ll (\bar{U}_+, \bar{C}_+),$$

where

$$\bar{C}_\pm = \kappa_1 \bar{U}_\pm,$$

and

$$0 < \bar{U}_- := \frac{\hat{\beta} - \sqrt{\hat{\beta}^2 - 4\hat{\chi}^2}}{2} < \bar{U}_+ := \frac{\hat{\beta} + \sqrt{\hat{\beta}^2 - 4\hat{\chi}^2}}{2}.$$

**Proposition 1** (Extinction) *Assume that  $R_1 < 1$ . Then the trivial equilibrium  $(0, 0)$  is globally asymptotically stable, that is,  $(0, 0)$  is locally stable and every nonnegative solution of (8) converges to  $(0, 0)$ .*

**Proof** We construct a family of upper solutions. For each  $\hat{U}_0 \geq 0$ , we fix  $\hat{C}_0 > 0$  such that

$$\hat{C}_0 = pe^{-\mu}\hat{C}_0 + pe^{-\mu} [1 - e^{-\alpha}] \hat{U}_0, \tag{15}$$

which is equivalent to

$$\hat{C}_0 = \frac{pe^{-\mu} [1 - e^{-\alpha}]}{1 - pe^{-\mu}} \hat{U}_0 = \kappa_1 \hat{U}_0,$$

and corresponds to the second equation of (8), which is possible since  $\mu > 0$ .

Define

$$\hat{f}(x) = \frac{\hat{\beta} x^2}{\hat{\chi}^2 + x^2} + e^{-(\mu+\alpha)x}.$$

which corresponds to the right-hand side of the first equation of (8) whenever  $C(n)$  and  $U(n)$  satisfy (15).

Let  $(\hat{U}(n), \hat{C}(n))$  be the solution (8) starting from  $(\hat{U}_0, \hat{C}_0)$ . Then,  $\hat{U}(1) = \hat{f}(\hat{U}(0)) < \hat{U}(0)$  and by construction  $\hat{C}(1) = \hat{C}(0)$ . Therefore,

$$\begin{cases} \hat{U}(1) = F(\hat{U}(0), \hat{C}(0)) < \hat{U}(0), \\ \hat{C}(1) = G(\hat{U}(0), \hat{C}(0)) = \hat{C}(0). \end{cases}$$

Since  $F$  and  $G$  are strictly increasing, the sequence  $(\hat{U}(n), \hat{C}(n))$  is decreasing and converges to the largest equilibrium below  $(\hat{U}_0, \hat{C}_0)$ , which is  $(0, 0)$ .

Now let  $(U_0, C_0) \in \mathbb{R}_+^2$ . We can choose  $\widehat{C}_0 > 0$  large enough and  $\widehat{U}_0$  satisfying (15) such that

$$\widehat{C}_0 \geq C_0 \text{ and } \widehat{U}_0 \geq U_0.$$

Since  $F$  and  $G$  are strictly increasing, for each integer  $n \geq 0$ , we have

$$\widehat{C}(n) \geq C(n) \text{ and } \widehat{U}(n) \geq U(n).$$

Since  $(\widehat{C}(n), \widehat{U}(n))$  converges to  $(0, 0)$ ,  $(\widehat{U}(n), \widehat{C}(n))$  converges to  $(0, 0)$ .

The local stability follows by using the same arguments. Indeed by choosing  $\widehat{C}_0 > 0$  small enough, we obtain a positively invariant neighborhood of  $(0, 0)$  in  $\mathbb{R}_+^2$  as small as we want.  $\square$

The proof of the following proposition is based on the same argument as the proof of Proposition 1.

**Proposition 2** *Assume that  $R_1 > 1$ . The following statements hold:*

- (i) *The equilibrium  $(0, 0)$  is asymptotically stable. If  $U_0 \in [0, \overline{U}_-)$  and  $C_0 \in [0, \overline{C}_-)$ , then the corresponding solution  $(U(n), C(n))$  of (8) converges to  $(0, 0)$ .*
- (ii) *The equilibrium  $(\overline{U}_+, \overline{C}_+)$  is asymptotically stable. If  $U_0 \in (\overline{U}_-, \infty)$  and  $C_0 \in (\overline{C}_-, \infty)$ , then the corresponding solution  $(U(n), C(n))$  of (8) converges to  $(\overline{U}_+, \overline{C}_+)$ .*

**Proof** The proof is similar to Proposition 1. For each fixed  $\widehat{U}(0) \geq 0$ , let  $\widehat{C}(0) = \kappa_1 \widehat{U}(0)$ . Let  $(\widehat{U}(n), \widehat{C}(n))$  be the solution (8) starting from  $(\widehat{U}_0, \widehat{C}_0)$ . If  $\widehat{U}_0 \in [0, \overline{U}_-)$   $\cup$   $(\overline{U}_+, \infty)$ , then  $\widehat{C}_0 \in [0, \overline{C}_-)$   $\cup$   $(\overline{C}_+, \infty)$  and

$$\begin{cases} \widehat{U}(1) = F(\widehat{U}(0), \widehat{C}(0)) < \widehat{U}(0), \\ \widehat{C}(1) = G(\widehat{U}(0), \widehat{C}(0)) = \widehat{C}(0). \end{cases}$$

Since  $F$  and  $G$  are strictly increasing, the sequence  $(\widehat{U}(n), \widehat{C}(n))$  is decreasing and converges to the largest equilibrium below  $(\widehat{U}_0, \widehat{C}_0)$ . If  $\widehat{U}_0 \in [0, \overline{U}_-)$ , this equilibrium is  $(0, 0)$ ; if  $\widehat{U}_0 \in (\overline{U}_+, \infty)$ , this equilibrium is  $(\overline{U}_+, \overline{C}_+)$ . Similarly, if  $\widehat{U}_0 \in (\overline{U}_-, \overline{U}_+)$ , then  $\widehat{C}_0 \in (\overline{C}_-, \overline{C}_+)$ , and the sequence  $(\widehat{U}(n), \widehat{C}(n))$  is increasing and converges to the smallest equilibrium above  $(\widehat{U}_0, \widehat{C}_0)$ , which is  $(\overline{U}_+, \overline{C}_+)$ .

For any  $(U_0, C_0) \in (0, \overline{U}_-) \times (0, \overline{C}_-)$ , we can find  $(\widehat{U}_0, \widehat{C}_0) \in (0, \overline{U}_-) \times (0, \overline{C}_-)$  with  $\widehat{C}(0) = \kappa_1 \widehat{U}(0)$  such that

$$\widehat{C}_0 \geq C_0 \text{ and } \widehat{U}_0 \geq U_0.$$

Since  $F$  and  $G$  are strictly increasing, we have  $\widehat{C}(n) \geq C(n)$  and  $\widehat{U}(n) \geq U(n)$ , and the sequence  $(\widehat{U}(n), \widehat{C}(n))$  converges to  $(0, 0)$ .

For any  $(U_0, C_0) \in (\overline{U}_-, \infty) \times (\overline{C}_-, \infty)$ , we can find  $(\widehat{U}_0, \widehat{C}_0) \in (\overline{U}_+, \infty) \times (\overline{C}_+, \infty)$  with  $\widehat{C}(0) = \kappa_1 \widehat{U}(0)$  such that  $\widehat{C}_0 \geq C_0$  and  $\widehat{U}_0 \geq U_0$ . We can also find  $(\check{U}_0, \check{C}_0) \in (\overline{U}_-, \overline{U}_+) \times (\overline{C}_-, \overline{C}_+)$  with  $\check{C}(0) = \kappa_1 \check{U}(0)$  such that  $\check{C}_0 \leq C_0$  and  $\check{U}_0 \leq$

$U_0$ . Then the sequence  $(\widehat{U}(n), \widehat{C}(n))$  is decreasing to  $(\overline{U}_+, \overline{C}_+)$ , and the sequence  $(\check{U}(n), \check{C}(n))$  is increasing to  $(\overline{U}_+, \overline{C}_+)$ . Since

$$\widehat{U}_0 \geq U_0 \geq \check{U}_0 \text{ and } \widehat{C}_0 \geq C_0 \geq \check{C}_0,$$

and  $F$  and  $G$  are strictly increasing, we have

$$\widehat{U}(n) \geq U(n) \geq \check{U}(n) \text{ and } \widehat{C}(n) \geq C(n) \geq \check{C}(n), \text{ for all } n \geq 0.$$

Therefore,  $(U(n), C(n))$  converges to  $(\overline{U}_+, \overline{C}_+)$ . □

In the case  $R_1 > 1$ , we can prove that the solution of (8) converges to  $(\overline{U}_+, \overline{C}_+)$  if either  $U_0$  is large enough or  $C_0$  is large enough.

**Proposition 3** *Assume that  $R_1 > 1$ . There exist  $M, N > 0$  such that for any  $(U_0, C_0)$  with  $U_0 \geq M$  or  $C_0 \geq N$ , the solution of (8) converges to  $(\overline{U}_+, \overline{C}_+)$ .*

**Proof** By Proposition 2, it suffices to show that there exist  $M, N > 0$  such that, for any  $(U_0, C_0)$  with  $U_0 \geq M$  or  $C_0 \geq N$ ,  $(U(n), C(n)) \in (\overline{U}_-, \infty) \times (\overline{C}_-, \infty)$  for some  $n \geq 0$ . The existence of  $M$  is obvious, as it suffices to set

$$M = \max \left\{ \frac{\overline{U}_-}{e^{-(\mu+\alpha)}} + 1, \frac{\overline{C}_-}{pe^{-\mu}(1 - e^{-\alpha})} + 1 \right\}.$$

If  $U_0 \geq M$ , then  $(U(1), C(1)) \in (\overline{U}_-, \infty) \times (\overline{C}_-, \infty)$ , and the solution  $(U(n), C(n))$  of (8) converges to  $(\overline{U}_+, \overline{C}_+)$ .

To see the existence of  $N$ , we consider a sequence  $\{x_n\}$  determined by the iteration  $x_{n+1} = \beta/2 + e^{-(\mu+\alpha)}x_n$  with  $x_0 = U_0$ . Since  $\{x_n\}$  converges to  $\hat{\beta}/2 > \overline{U}_-$ , there exists  $K > 0$  such that  $x_K > \overline{U}_-$ . Since  $C(n+1) \geq pe^{-\mu}C(n)$  and  $V(n) \geq pe^{-\mu}C(n)$ , there exists  $N > 0$  such that if  $C_0 \geq N$ , then we have  $C(n) > \overline{C}_-$  and

$$\frac{\beta V(n)^2}{\chi^2 + V(n)^2} \geq \frac{\beta}{2}$$

for all  $1 \leq n \leq K$ . So, for all  $(U_0, C_0)$  with  $C_0 \geq N$ , we have  $U(n+1) \geq \beta/2 + e^{-(\mu+\alpha)}U(n)$ ,  $1 \leq n \leq k$ . Then,  $U(n) \geq x_n$  for all  $1 \leq n \leq K$ , and therefore,  $U(K) \geq x_K > \overline{U}_-$ . Hence,  $(U(K), C(K)) \in (\overline{U}_-, \infty) \times (\overline{C}_-, \infty)$ . □

### 3.2 Case $p = 1$

In the case  $p = 1$ , the difference equation (8) becomes

$$\begin{cases} U(n+1) = \frac{\beta (e^{-\mu}(U(n) + C(n)))^2}{\chi^2 + (e^{-\mu}(U(n) + C(n)))^2} + e^{-(\mu+\alpha)}U(n), \\ C(n+1) = e^{-\mu}C(n) + e^{-\mu} [1 - e^{-\alpha}]U(n), \end{cases} \tag{16}$$

with initial distribution

$$U(0) = U_0 \geq 0 \text{ and } C(0) = C_0 \geq 0.$$

By summing the two equations of (16), we have

$$U(n + 1) + C(n + 1) = g(e^{-\mu} [U(n) + C(n)]) + e^{-\mu} [U(n) + C(n)]$$

and we deduce the following result:

**Proposition 4** Assume that  $p = 1$  and  $R_1 > 1$ . The following hold:

(i) The equilibrium  $(0, 0)$  is locally asymptotically stable. Moreover, the domain

$$D^- = \left\{ (U, C) \in \mathbb{R}_+^2 : U + C < \bar{U}_- + \bar{C}_- \right\}$$

is positively invariant for (8). Furthermore, every solution of (8) starting on  $D^+$  (i.e. with  $U_0 + C_0 < \bar{U}_- + \bar{C}_-$ ) converges to  $(0, 0)$ .

(ii) The equilibrium  $(\bar{U}_+, \bar{C}_+)$  is locally asymptotically stable. Moreover, the domain

$$D^+ = \left\{ (U, C) \in \mathbb{R}_+^2 : U + C > \bar{U}_- + \bar{C}_- \right\}$$

is positively invariant for (8). Furthermore, every solution of (8) starting on  $D^+$  (i.e. with  $U_0 + C_0 > \bar{U}_- + \bar{C}_-$ ) converges to  $(\bar{U}_+, \bar{C}_+)$ .

(iii) The equilibrium  $(\bar{U}_-, \bar{C}_-)$  is unstable. Moreover, the separatrix between  $D^-$  and  $D^+$  is

$$S = \left\{ (U, C) \in \mathbb{R}_+^2 : U + C = \bar{U}_- + \bar{C}_- \right\},$$

which has slope  $-1$  and is positively invariant for (8). Furthermore, every solution of (8) starting on  $S$  (i.e. with  $U_0 + C_0 = \bar{U}_- + \bar{C}_-$ ) converges to  $(\bar{U}_-, \bar{C}_-)$ .

**Remark 1** We remark that if  $p = 1$ , then  $\bar{U}_-$  is a decreasing function of  $\alpha$  and  $\bar{U}_+$  is an increasing function of  $\alpha$ . Further, if  $p = 1$  and  $\alpha \geq 0$ , then  $R_0$  (in the case without contamination) =  $R_1$  (in the case with contamination), and  $\bar{U}_-$  (in the case without contamination) =  $\bar{U}_- + \bar{C}_-$  in the case with contamination. The same equality holds for  $\bar{U}_+$  and  $\bar{C}_+$ .

### 3.3 Case $p < 1$

The following result compares the system (8) with the system (16).

**Lemma 3** (Comparison property) If  $(U(n), V(n))$  is a solution of (8) starting from  $(U(0), V(0)) \in [0, \infty)^2$ , then

$$(U(n), V(n)) \leq (\tilde{U}(n), \tilde{V}(n)), \forall n \geq 0,$$

where  $(\tilde{U}(n), \tilde{V}(n))$  is the solution of (16) starting from the same initial value. Let  $(\bar{U}_-, \bar{C}_-)$  be the smallest positive equilibrium of (16) corresponding to  $p = 1$ . Then, each solution of (8) starting from an initial value satisfying  $U_0 + C_0 < \bar{U}_- + \bar{C}_-$  converges to  $(0, 0)$ .

**Proof** In order to prove the above result, it is sufficient to observe that

$$V(0) := U(1^-) + pC(1^-) = e^{-(\mu+\alpha)}U_0 + p \left( e^{-\mu}C_0 + \left[ e^{-\mu} - e^{-(\alpha+\mu)} \right] U_0 \right),$$

and since  $p \in [0, 1]$ , we deduce that

$$V(0) \leq U(1^-) + C(1^-) = e^{-\mu}(U_0 + C_0).$$

It follows that  $U(1) \leq \tilde{U}(1)$  and  $C(1) \leq \tilde{C}(1)$ . Then,

$$V(1) \leq e^{-\mu}(U(1) + C(1)) \leq e^{-\mu}(\tilde{U}(1) + \tilde{C}(1)),$$

and it follows that  $U(2) \leq \tilde{U}(2)$  and  $C(2) \leq \tilde{C}(2)$ . By induction, we have  $(U(n), V(n)) \leq (\tilde{U}(n), \tilde{V}(n))$  for all  $n \geq 0$ . If  $U_0 + C_0 < \bar{U}_- + \bar{C}_-$ , then the sequence  $\tilde{U}(n) + \tilde{V}(n)$  converges to 0 by Proposition 4. Therefore,  $(U(n), V(n))$  converges to  $(0, 0)$ .  $\square$

**Theorem 1** (Allee effect) *Assume that  $R_1 > 1$ , and let  $(\bar{U}_-, \bar{C}_-)$  be the smallest positive equilibrium of (16). For each  $\tilde{U} > 0$  and  $\tilde{C} > 0$ , there exists a constant  $\alpha_0 > 0$ , which depends on  $(\tilde{U}, \tilde{C})$ , such that*

$$\alpha_0(\tilde{U} + \tilde{C}) \geq \bar{U}_- + \bar{C}_-$$

where  $(\bar{U}_-, \bar{C}_-)$  is the smallest positive equilibrium of (16) corresponding to  $p = 1$ . Moreover, the following alternatives hold:

- (i) If  $\alpha < \alpha_0$  the solution of (8) starting from  $(U_0, C_0) = (\alpha\tilde{U}, \alpha\tilde{C})$  converges to  $(0, 0)$ .
- (ii) If  $\alpha > \alpha_0$  the solution of (8) starting from  $(U_0, C_0) = (\alpha\tilde{U}, \alpha\tilde{C})$  persists and the sum  $U(n) + C(n)$  stays above  $\bar{U}_- + \bar{C}_-$  for each integer  $n \geq 0$ .

**Proof** For any  $\tilde{U}, \tilde{C} > 0$  and  $(U_0, C_0) = (\alpha\tilde{U}, \alpha\tilde{C})$ , we observe that if  $\alpha\tilde{U} + \alpha\tilde{C} < \bar{U}_- + \bar{C}_-$ ,  $(U(n), C(n))$  converges to  $(0, 0)$  by Lemma 3. By the monotonicity of the system, we observe that, for any  $0 < \alpha' < \alpha''$ , if the solution with initial data  $(\alpha''\tilde{U}, \alpha''\tilde{C})$  converges to  $(0, 0)$ , the solution with initial data  $(\alpha'\tilde{U}, \alpha'\tilde{C})$  converges to  $(0, 0)$ .

Define  $\alpha_0 =$

$$\sup\{\alpha > 0 : (U(n), C(n)) \text{ with initial data } (\alpha\tilde{U}, \alpha\tilde{C}) \text{ converges to } (0, 0)\}.$$

By our previous observations,  $\alpha_0 > 0$  is well defined and  $\alpha_0(\tilde{U} + \tilde{C}) \geq \bar{U}_- + \bar{C}_-$ . Since, if  $\alpha$  is large, the solution converges to the positive equilibrium, we have  $\alpha_0 < \infty$ .

If  $\alpha > \alpha_0$ ,  $(U(n), C(n))$  does not converge to  $(0, 0)$ , and we must have  $U(n) + C(n) \geq \bar{U}_-^* + \bar{C}_-^*$  for  $n \geq 0$  by Lemma 3. □

**Theorem 2** Assume that  $R_1 \geq 1$ . For each  $\tilde{U} > 0$  and  $\tilde{C} > 0$ , there exists a constant  $\alpha_1 > \alpha_0$ , which depend on  $(\tilde{U}, \tilde{C})$ , such that the following hold:

(i) If  $\alpha < \alpha_1$  the solution of (8) starting from  $(U_0, C_0) = (\alpha\tilde{U}, \alpha\tilde{C})$  stays away from the largest positive equilibrium of (8). More precisely, there exists  $\varepsilon > 0$ , independent of  $\alpha$ , such that

$$\|(U(n) - \bar{U}_+, C(n) - \bar{C}_+)\| \geq \varepsilon, \forall n \geq 0.$$

(ii) If  $\alpha > \alpha_1$  the solution of (8) starting from  $(U_0, C_0) = (\alpha\tilde{U}, \alpha\tilde{C})$  converges to  $(\bar{U}_+, \bar{C}_+)$ .

**Proof** By the monotonicity of the system, we observe that, for any  $0 < \alpha' < \alpha''$ , if the solution of (8) with initial data  $(\alpha'\tilde{U}, \alpha'\tilde{C})$  converges to  $(\bar{U}_+, \bar{C}_+)$ , the solution of (8) with initial data  $(\alpha''\tilde{U}, \alpha''\tilde{C})$  converges to  $(\bar{U}_+, \bar{C}_+)$ . Moreover, we observe that, for each  $\tilde{U} > 0$  and  $\tilde{C} > 0$ , the solution of (8) with initial data  $(\alpha\tilde{U}, \alpha\tilde{C})$  converges to  $(\bar{U}_+, \bar{C}_+)$  if  $\alpha$  is large enough by Proposition 2.

Define  $\alpha_1 =$

$$\inf\{\alpha > 0 : (U(n), C(n)) \text{ with initial data } (\alpha\tilde{U}, \alpha\tilde{C}) \text{ converges to } (\bar{U}_+, \bar{C}_+)\}.$$

By our previous observations,  $\alpha_1 > \alpha_0$  is well defined, where  $\alpha_0$  is given by Theorem 1. By the definition of  $\alpha_1$ , (ii) is true. (i) follows from the fact that if  $(U(n), C(n)) \in (\bar{U}_-, \infty) \times (\bar{C}_-, \infty)$  for some  $n \geq 0$ , then the sequence  $(U(n), C(n))$  converges to  $(\bar{U}_+, \bar{C}_+)$ . □

## 4 Numerical Simulations

We illustrate the behavior of the solutions of model (8) with numerical simulations. Model (8) is of the form

$$\begin{cases} U(n+1) = F(U(n), C(n)), \\ C(n+1) = G(U(n), C(n)), \end{cases}$$

(see 9), where  $F$  and  $G$  are strictly increasing functions (see (10) and (11)). By the monotonicity of  $F$  and  $G$ , the sequence  $\{(U(n), C(n))\}$  with initial data  $(U_0, C_0)$  satisfying

$$\begin{cases} U \leq F(U, C) \\ C \leq G(U, C) \end{cases} \tag{17}$$

is increasing. Similarly, the sequence  $\{(U(n), C(n))\}$  with initial data  $(U_0, C_0)$  satisfying (17) with both inequalities reversed is decreasing.

The parameters in the first simulation of Model (8) are given in Table 1.

**Table 1** Parameters and steady states for forager bees in the simulation

Parameter/ equilibrium	Simulation value	References
$\mu$	.1/day	Betti et al. (2014), DeGrandi-Hoffman and Curry (2004), Dukas (2008), Henry et al. (2012), Henry et al. (2015), Khoury et al. (2011), Myerscough et al. (2017) and Torres et al. (2015)
$\alpha$	.03/day	Henry et al. (2012, 2015)
$\beta$	2900	Truitt et al. (2019)
$\chi$	11,000	Betti et al. (2014), Dennis and Kemp (2016), Kang and Theraulaz (2016), Kang et al. (2016) and Truitt et al. (2019)
$p$	.8	Henry et al. (2012, 2015)
$(\bar{U}_+, \bar{C}_+)$	(14,889 , 1154)	DeGrandi-Hoffman et al. (1989), DeGrandi-Hoffman and Curry (2004), Dennis and Kemp (2016), Khoury et al. (2011) and vanEngelsdorp et al. (2009)
$(\bar{U}_-, \bar{C}_-)$	(8900, 690)	DeGrandi-Hoffman et al. (1989), DeGrandi-Hoffman and Curry (2004), Dennis and Kemp (2016), Khoury et al. (2011) and vanEngelsdorp et al. (2009)

$\mu$  = daily mortality rate of uncontaminated foragers and contaminated foragers (including normal homing failure),  $\beta$  = production parameter in the daily output of new uncontaminated foragers,  $\chi$  = Allee parameter in the daily output of new uncontaminated foragers,  $1 - p$  = fraction of contaminated bees failing to return back to the hive each day (in addition to normal homing failure),  $\alpha$  = daily rate of contamination of uncontaminated bees,  $(\bar{U}_+, \bar{C}_+)$  = locally stable steady state,  $(\bar{U}_-, \bar{C}_-)$  = locally unstable steady state

In the simulation,  $R_1 = 1.0333 > 1$ . Figure 2 provides a phase portrait of the solutions, where the dots indicate  $U$  and  $C$  values each day. In Fig. 2, the points satisfying (17) are in the yellow region, which is invariant. If the initial value  $(U_0, C_0)$  is in the yellow region,  $\{(U(n), C(n))\}$  is increasing and convergent to the equilibrium  $(\bar{U}_+, \bar{C}_+)$ . The initial data satisfying (17) with the inequalities reversed are in the gray and red regions, which are also invariant. If the initial value is in the gray region,  $\{(U(n), C(n))\}$  is decreasing and convergent to the equilibrium  $(0, 0)$ ; if the initial value is in the red region,  $\{(U(n), C(n))\}$  is decreasing and convergent to the equilibrium  $(\bar{U}_+, \bar{C}_+)$ .

The equilibria and the three regions are determined as follows: Solve the equation  $G(U, C) = C$  for  $C$  and obtain the line  $C_1(U) = \kappa_1 U$ , where  $\kappa_1 = 0.0775$ . Since  $R_1 > 1$ , there are three equilibria  $0, (\bar{U}_-, \bar{C}_-), (\bar{U}_+, \bar{C}_+)$ . Solve the equation  $F(U, \kappa_1 U) = U$  for  $U$  and obtain the three values  $0 < \bar{U}_- < \bar{U}_+$ . Set  $\bar{C}_- = \kappa_1 \bar{U}_-$ , and  $\bar{C}_+ = \kappa_1 \bar{U}_+$ . Solve the equation  $F(U, C) = U$  for  $C$  and obtain two roots  $C_{\pm}(U) =$



$$\frac{29560.6 U - 1.24261 U^2 \pm 4.38501 \sqrt{(2.85694 \times 10^{11} - 1.20094 \times 10^7 U) U}}{23789.1 - U}$$

Set  $C_2(U) = C_+(U)$ . The intersection of  $C_1(U)$  and  $C_2(U)$  yields the three regions and the equilibria  $(\bar{U}_-, \bar{C}_-)$  and  $(\bar{U}_+, \bar{C}_+)$ .

We conjecture that there are two separatrices dividing  $\mathbb{R}_+^2$  into the invariant regions and the regions of attractions for the equilibria  $(0, 0)$ ,  $(\bar{U}_-, \bar{C}_-)$ , and  $(\bar{U}_+, \bar{C}_+)$ , that are almost straight lines. We have numerically verified this conjecture for the this simulation and other simulations. We call these approximating lines Separatrix 1 and Separatrix 2, respectively. The approximating slopes of Separatrix 1 and Separatrix 2 are determined as follows: Obtain the linearization of  $F(U, C) - U$  and  $G(U, C) - C$ :

$$J(U, C) = \begin{bmatrix} \frac{\partial F(U, C) - U}{\partial U} & \frac{\partial F(U, C) - U}{\partial C} \\ \frac{\partial G(U, C) - C}{\partial U} & \frac{\partial G(U, C) - C}{\partial C} \end{bmatrix}.$$

The linearization  $J[\bar{U}_-, \bar{C}_-]$  yields the eigenvalues  $1.029 > 1.0$  and  $.7158 < 1.0$ , which indicates a saddle point. Their eigenvectors are, respectively,

$$\begin{bmatrix} .9976 \\ .0698 \end{bmatrix} \text{ (slope} = -2.647), \quad \begin{bmatrix} -.3534 \\ .9355 \end{bmatrix} \text{ (slope} = .0699).$$

The linearization  $J[\bar{U}_+, \bar{C}_+]$  yields the eigenvalues  $.9699 < 1$  and  $.7178 < 1$ , which indicates a stable node. Their eigenvectors are, respectively,

$$\begin{bmatrix} .9962 \\ .0866 \end{bmatrix} \text{ (slope} = .0869), \quad \begin{bmatrix} -.2703 \\ .9628 \end{bmatrix} \text{ (slope} = -3.562).$$

The approximations to Separatrix 1 and Separatrix 2 in Fig. 2 are straight lines with slopes  $-2.647$  and  $-3.562$ , respectively. These linearizations yield the local behavior of the solutions at the equilibria, as graphed in Fig. 3.

In the numerical illustrations below, we examine the behavior of the solutions of (8) in terms of the homing failure parameter  $p$  and the contamination rate parameter  $\alpha$ . In Fig. 4, we graph  $R_1(p, \alpha)$  as a function of  $p$  and  $\alpha$ . The parameters  $\beta, \chi,$  and  $\mu$  are as in Table 1.

In Fig. 5, we plot the values of the equilibria  $\bar{U}_-$  and  $\bar{C}_-$  as the contaminated homing failure parameter  $p$  and the contamination rate parameter  $\alpha$  vary. The parameters  $\beta, \chi, \mu$  are as in Table 1.

In Figs. 6 and 7, we plot the phase portraits of the solutions as the contaminated homing failure parameter  $p$  and the contamination rate parameter  $\alpha$  vary. The parameters  $\beta, \chi, \mu$  are as in Table 1.

In our last numerical illustration, we alter the initial values  $U_0$  and  $C_0$ . If the total initial population  $U_0 + C_0$  is sufficiently high, CCD is avoided. If not, CCD occurs. The parameters  $\beta, \chi, \mu, p, \alpha$  are as in Table 1 (Fig. 8).

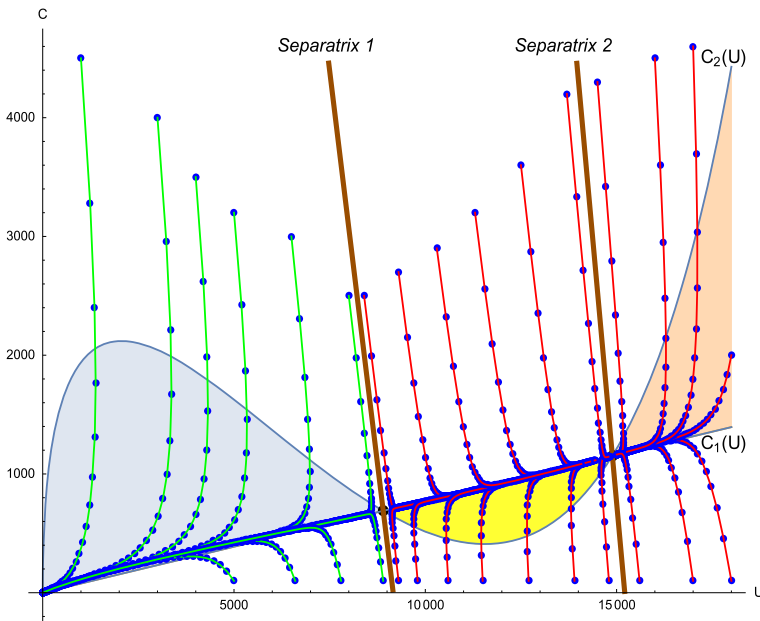


**Fig. 2** The parameters are  $\beta = 2900$ ,  $\chi = 11,000$ ,  $\mu = 0.1$ ,  $\alpha = 0.03$ , and  $p = .8$ .  $R_1 = 1.0333$ . Separatrix 1 is, approximately, a straight line with slope  $-2.65$ . Separatrix 2 is, approximately, a straight line with slope  $-3.56$ . The dots correspond to daily values. The three intersection points of  $C_1(U)$  and  $C_2(U)$  are the equilibria of (8), and the three colored regions are invariant with respect to (8). If the initial value is in the yellow region,  $U(n)$  and  $C(n)$  are increasing. If the initial value is in the gray or red region,  $U(n)$  and  $C(n)$  are decreasing. The equilibria  $(0, 0)$  and  $(\bar{U}_+, \bar{C}_+)$  are locally stable, and  $(\bar{U}_-, \bar{C}_-)$  is unstable (Color figure online)

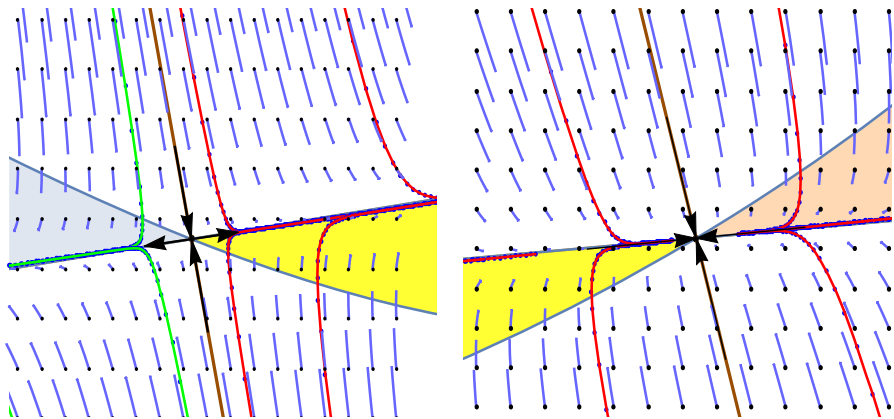


**Fig. 3** The regions in Fig. 2 surrounding the equilibria  $(\bar{U}_-, \bar{C}_-)$  (left) and  $(\bar{U}_+, \bar{C}_+)$  (right). The black arrows are obtained from the eigenvalues and eigenvectors of the linearization of  $\{F(U, C) - U, G(U, C) - C\}$  at the equilibria, and define the approximating separatrices. The black dots are initial values. The blue lines are the movement in one day (Color figure online)

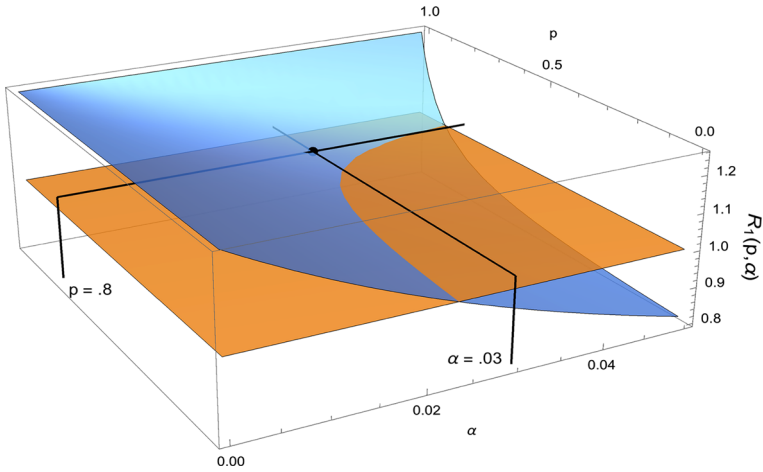


**Fig. 4**  $R_1(p, \alpha)$  as a function of  $p$  and  $\alpha$ .  $R_1(p, \alpha)$  decreases more sharply as  $p$  decreases, than as  $\alpha$  increases. If  $p = 1$ , then  $R_1(1, \alpha) = 1.253$ , independent of  $\alpha$  (Color figure online)

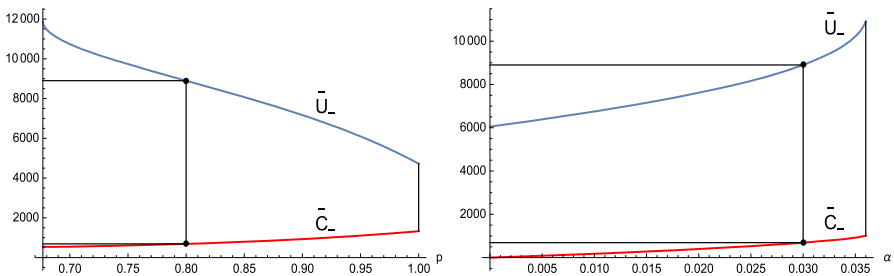


**Fig. 5** The equilibria  $\bar{U}_-$  and  $\bar{C}_-$  of (8) as  $p$  and  $\alpha$  vary. Left:  $\alpha = .03$ ,  $p \in (0.6768, 1.0)$ . For  $p < 0.6768$ , only the  $(0, 0)$  equilibrium exists. Right:  $p = 0.8$ ,  $\alpha \in (0.0, 0.0362)$ . For  $\alpha > 0.0362$ , only the  $(0, 0)$  equilibrium exists (Color figure online)

### 5 Conclusions

Honey bee colony collapse disorder (CCD) is a serious ecological and agricultural problem throughout the world, and much further research is needed to understand its causation and prevention. In this paper, we have focused on environmental pesticide contamination (EPC) as a major instigator of honey bee CCD. The role of pesticides in CCD is highly controversial, and the restriction of pesticides has been proposed and opposed in current scientific research and government legislation. The extensive use of pesticides in industrial agriculture is very important in agricultural economics, and its constraint has serious economic impact. Many studies have suggested limited impact of EPC on CCD and provide opposition to constraints on agricultural pesticide use. Other studies identify significant impact of EPC on CDD and provide strong advocacy for such constraints.

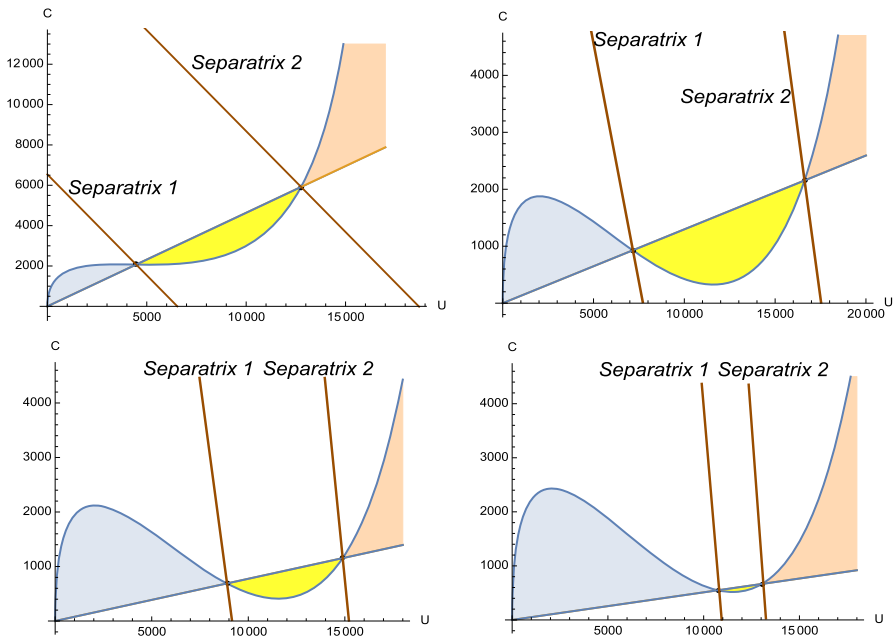


**Fig. 6** Slopes of the separatrices as  $p$  changes. Top left:  $p = 1.0$ , both slopes are  $-1$ . Top right  $p = .9$ , Separatrix 1 slope =  $-1.68$ , and Separatrix 2 slope =  $-2.36$ . Bottom left:  $p = .8$ , Separatrix 1 slope =  $-2.65$ , and Separatrix 2 slope =  $-3.56$ . Bottom right:  $p = .7$ , Separatrix 1 slope =  $-4.19$ , and Separatrix 2 slope =  $-4.80$ . The slopes are increasingly negative as  $p$  decreases (Color figure online)

We have designed a mathematical model of pesticide contamination in honey bee environments that quantifies the capacity of EPC to generate CCD and provides understanding and resolution for this controversy.

Our model has three key features:

1. Honey bee colonies have a critical population viability threshold, below which their population rapidly disintegrates, but above which their population approaches a stable level. This feature of our model is incorporated as an Allee effect, which is based on a sustainable level of production of younger bees in the hive to offset the mortality of forager bees outside the hive.
2. EPC has sub-lethal effect on forager honey bees and does not directly cause CCD. Rather, the effect of EPC on forager bees is to impair the capacity of contaminated forager bees to return home each day, which disrupts their essential social contribution to the sustenance of younger bees in the hive.
3. The level of daily homing failure in contaminated forager bees is quantifiable in terms of the population viability threshold and can be overcome if the total population of both uncontaminated and contaminated forager bees is sufficiently high.

CCD is a complex phenomenon, which may have multifactorial causes, difficult to appraise scientifically. Studies that do not show significant connection of EPC to CCD may be cases in which EPC does not cause the population to fall below the crit-

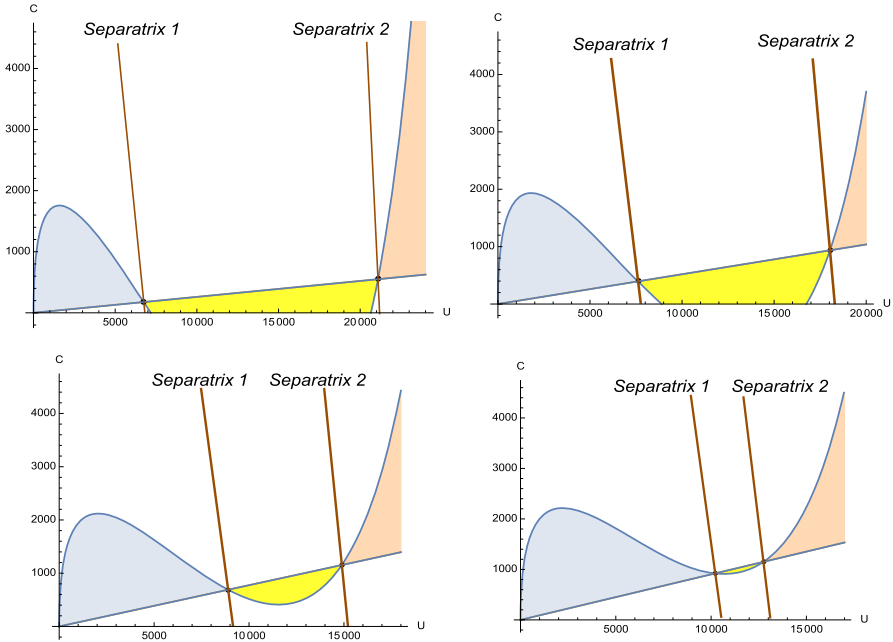


**Fig. 7** Slopes of the separatrices as  $\alpha$  changes. Top left:  $\alpha = 0.1$ , Separatrix 1 slope =  $-2.66$ , and Separatrix 2 slope =  $-5.62$ . Top right  $\alpha = 0.2$ , Separatrix 1 slope =  $-2.62$ , and Separatrix 2 slope =  $-4.46$ . Bottom left:  $\alpha = 0.3$ , Separatrix 1 slope =  $-2.65$ , and Separatrix 2 slope =  $-3.56$ . Bottom right:  $\alpha = 0.35$ , Separatrix 1 slope =  $-2.75$ , and Separatrix 2 slope =  $-3.11$  (Color figure online)

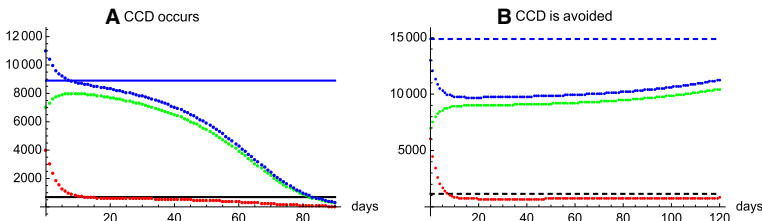


**Fig. 8** Graphs of  $U(n)$  (green),  $C(n)$  (red), and  $U(n) + C(n)$  (blue). The dots represent daily values. A:  $\bar{U}_- = 8900.01$  (blue line),  $\bar{C}_- = 689.54$  (black line).  $U_0 = 7000$ ,  $C_0 = 4000$ , total initial population =  $11,000$ . The total population decreases rapidly below the viable threshold  $8900.01$ . B:  $U_0 = 7000$ ,  $C_0 = 6000$ , total initial population =  $13,000$ . The populations  $U(n)$  and  $C(n)$  increase gradually to the limiting values  $\bar{U}_+ = 14,889.1$  (blue dashed line),  $\bar{C}_+ = 1153.55$  (black dashed line), respectively (Color figure online)

ical viability threshold, whereas studies that show a connection may have population loss below this threshold. Consequently, the reduction of CCD, in managed honey bee colonies, may be accomplished by decreasing pesticide use in their agricultural environments and also by hive managers increasing hive population sizes to above threshold values.

**Acknowledgements** The authors express thanks to Dr. Frederic Barraquand, CNRS, IMB Bordeaux, France, for helpful assistance in the biological background of this work.

## Compliance with Ethical Standards

**Conflict of interest** The authors declare that they have no conflict of interest.

## References

- Abou-Shaara HF (2014) The foraging behaviour of honey bees, *Apis mellifera*: a review. *Vet Med* 59(1):1–10
- American Society for Horticultural Science, U.S. states begin ban on neonicotinoids (2019) <https://ashs.org/blogpost/1288786/251171/>
- Banks HT, Banks JE, Bommarco R et al (2017) Modeling bumble bee population dynamics with delay differential equations. *Ecol Model* 351:14–23
- Barron AB (2015) Death of the bee hive: understanding the failure of an insect society. *Sci Direct* 10:45–50
- Becher MA, Osborne JL, Thorbek P et al (2013) Towards a systems approach for understanding honeybee decline: a stocktaking and synthesis of existing models. *J Appl Ecol* 50:868–880
- Becher MA, Grimm V, Thorbek P et al (2014) BEEHAVE: a systems model of honeybee colony dynamics and foraging to explore multifactorial causes of colony failure. *J Appl Ecol* 51:470–482
- Becher MA, Twiston-Davies G, Penny TD (2018) Bumble-BEEHAVE: a systems model for exploring multifactorial causes of bumblebee decline at individual, colony, population and community level. *J Appl Ecol* 55:2797–2801
- Bee Informed Partnership, Total US managed honey bee colonies loss estimates (2018) <https://beeinformed.org>
- Bernardi S, Venturino E (2016) Viral epidemiology of the adult *Apis Mellifera* infested by the Varroa destructor mite. *Sci Direct* 5:e00101
- Betti MI, Wahl LM, Zamir M (2014) Effects of infection on honey bee population dynamics: a model. *PLoS ONE* 9(10):e110237
- Betti M, LeClair J, Wahl LM et al (2017) Bee++: an object-oriented, agent-based simulator for honeybee colonies. *Pop Sci* 8:31
- Blacquière T, Smagghe G, van Gestel CAM et al (2016) Neonicotinoids in bees: a review on concentrations, side-effects and risk assessment. *Ecotoxicology* 21(4):973–992
- Booten RD, Iwasa Y, Marshall JAR et al (2017) Stress-mediated Allee effects can cause the sudden collapse of honey bee colonies. *J Theor Biol* 420:213–219
- Bryden J, Gill RJ, Mitton RAA et al (2013) Chronic sublethal stress causes bee colony failure. *Ecol. Lett* 16:1463–1469
- Chauzat M-P, Carpentier P, Martel A-C et al (2009) Influence of pesticide residues on honey bee (Hymenoptera: Apidae) colony health in France. *Environ Entomol* 38(3):514–543
- Cutler GC, Scott-Dupree CD (2007) Exposure to clothianidin seed-treated canola has no long-term impact on honey bees. *J Econ Entomol* 100(3):765–772
- Cutler GC, Scott-Dupree CD, Sultan M et al (2014) A large-scale field study examining effects of exposure to clothianidin seed-treated canola on honey bee colony health, development, and overwintering success. *Peer J* 2:e652
- Cutler GC, Scott-Dupree CD (2016) A field study examining the effects of exposure to neonicotinoid seed-treated corn on commercial bumble bee colonies. *Ecotoxicology* 23(9):1755–1763
- DeGrandi-Hoffman G, Roth SA, Loper GL, Erickson EH (1989) BEEPOP: a honeybee population dynamics simulation model. *Ecol Model* 45:133–150
- DeGrandi-Hoffman G, Curry R et al (2004) A mathematical model of Varroa mite (*Varroa destructor* Anderson and Trueman) and honeybee *Apis mellifera* L. population dynamics. *Int J Acarol* 30(3):259–274
- Dennis B, Kemp WP (2016) How hives collapse: Allee effects, ecological resilience, and the honey bee. *PLoS ONE* 11(2):e0150055
- Desneux N, Decourtye A, Delpuech JM (2007) The sublethal effects of pesticides on beneficial arthropods. *Annu Rev Entomol* 52:81–106

- Dively GP, Embrey MS, Kamel A et al (2015) Assessment of chronic sublethal effects of imidacloprid on honey bee colony health. *PLoS ONE* 10:e0118748
- Dukas R (2008) Mortality rates of honey bees in the wild. *Insectes Sociaux* 55(3):252–255
- European Food Safety Authority, Neonicotinoids: risks to bees confirmed (2018) <https://doi.org/10.2903/sp.efsa.2018.EN-1378>
- European Food Safety Authority, Evaluation of the data on clothianidin, imidacloprid and thiamethoxam for the updated risk assessment to bees for seed treatments and granules in the EU (2018) <https://doi.org/10.2903/sp.efsa.2018.EN-1378>
- Farley JD (2017) Evolutionary dynamics of bee colony collapse disorder: steps toward a mathematical model of the contagion hypothesis. *J Adv Agric* 7(2):1050–1056
- Gabriellini G (2017) Seasonal effects on honey bee population dynamics: a nonautonomous system of difference equations. *Int J Differ Equ* 12(2):211–233
- Goulson D, Nicholls E, Botas C, Rotheray EL (2015) Bee declines driven by combined stress from parasites, pesticides, and lack of flowers. *Science* 347:1255957
- H.R. 3040-Saving America's Pollinators Act of 2017 (2018) <https://www.congress.gov/bill/115th-congress/house-bill/3040/text>
- Henry M, Béguin M, Requier F et al (2012) A common pesticide decreases foraging success and survival in honey bees. *Science* 336(6079):348–350
- Henry M, Cerrutti N, Aupinel P et al (2015) Reconciling laboratory and field assessments of neonicotinoid toxicity to honeybees. *Proc R Soc B Sci* 282:20152110
- Huang ZY, Robinson GE (1974) Regulation of honey bee division of labor by colony age demography. *Behav Ecol Sociobiol* 39:147–158
- Kang Y, Theraulaz G (2016) Dynamical models of task organization in social insect colonies. *Bull Math Biol* 78(5):879–915
- Kang Y, Blanco K, Davis T, Wang Y, DeGrandi-Hoffman G (2016) Disease dynamics of honeybees with Varroa destructor as parasite and virus vector. *Math Biosci* 275:71–92
- Khoury DS, Myerscough MR, Barron AB (2011) A quantitative model of honey bee colony population dynamics. *PLoS ONE* 6(4):e18491
- Krisbs-Zaleta CM, Mitchell C (2014) Modeling colony collapse disorder in honeybees as a contagion. *Math Biosci Eng* 11(6):1275–1294
- Leoncini I, Le Conte Y, Costagliola G et al (2004) Regulation of behavioral maturation by a primer pheromone produced by adult worker honey bees. *Proc Nat Acad Sci* 101:17559–17564
- Martin SJ (2002) The role of Varroa and viral pathogens in the collapse of honeybee colonies: a modeling approach. *J Appl Ecol* 38:1082–1093
- Meikle WG, Adamczyk JJ, Weiss M et al (2016) Sublethal effects of imidacloprid on honey bee colony growth and activity at three sites in the US. *PLoS ONE* 11:e0168603
- Myerscough MR, Khoury DS, Ronzani S, Barron AB (2017) Why do hives die? Using mathematics to solve the problem of honey bee colony collapse. In: Anderssen B et al (eds) *The role and importance of mathematics in innovation. Mathematics for industry*, vol 25. Springer, Singapore
- Nguyen BK, Saegerman C, Picard C et al (2009) Does imidacloprid seed-treated maize have an impact on honey bee mortality? *J Econ Entomol* 102(2):616–623
- Pilling E, Cambell E, Coulson M et al (2013) A four-year field program investigating long-term effects of repeated exposure of honey bee colonies to flowering crops treated with thiamethoxam. *PLoS ONE* 8:e77193
- Ratti V, Kevan PG, Eberl HJ (2013) A mathematical model for population dynamics in honeybee colonies infested with Varroa destructor and the acute bee paralysis virus. *Can Appl Math Q* 21(1):63–93
- Ratti V, Kevan PG, Eberl HJ (2015) A mathematical model of the honeybee-Varroa destructor-Acute bee paralysis virus system with seasonal effects. *Bull Math Biol* 77(8):1493–1520
- Ratti V, Kevan PG, Eberl HJ (2017) A mathematical model of forager loss in honeybee colonies infested with Varroa destructor and the acute bee paralysis virus. *Bull Math Biol* 79(6):1218–1253
- Rolke D, Fuchs S, Grunewald B et al (2016) Large-scale monitoring of effects of clothianidin-dressed oilseed rape seeds on pollinating insects in Northern Germany: effects on honey bees (*Apis mellifera*). *Ecotoxicology* 25(9):1648–1665
- Rundlof M, Andersson GKS, Bommarco R et al (2015) Seed coating with a neonicotinoid insecticide negatively affects wild bees. *Nature* 521:77–80
- Russell S, Barron AB, Harris D (2013) Dynamic modelling of honey bee (*Apis mellifera*) colony growth and failure. *Ecol Model* 265(10):158–169

- Sandrock C, Tanadini LG, Pettis JS et al (2014) Sublethal neonicotinoid insecticide exposure reduces solitary bee reproductive success. *Agric For Entomol* 16:119–128
- Schmickl T, Crailsheim K (2007) HoPoMo: a model of honeybee intracolony population dynamics and resource management. *Ecol Model* 204:219–245
- Schneider CW, Tautz J, Grünewald B et al (2012) RFID tracking of sublethal effects of two neonicotinoid insecticides on the foraging behavior of *Apis mellifera*. *PLoS ONE* 7(1):e30023
- Stanley DA, Russell AL, Morrison SJ et al (2016) Investigating the impacts of field-realistic exposure to a neonicotinoid pesticide on bumblebee foraging, homing ability and colony growth. *J Appl Ecol* 53:1440–1449
- Sumpter DJ, Martin SJ (2004) The dynamics of virus epidemics in Varroa-infested honey bee colonies. *J Animal Ecol* 73(1):51–63
- Thompson HM, Wilkins S, Harkin S et al (2015) Neonicotinoids and bumblebees (*Bombus terrestris*): effects on nectar consumption in individual workers. *Pest Manag Sci* 71(7):946–950
- Torres DJ, Ricoy UM, Roybal S (2015) Modeling honey bee populations. *PLoS ONE* 10(7):e0130966
- Truitt LL, McArt SH, Vaughn AH, Ellner SP (2019) Trait-based modeling of multihost pathogen transmission: plant-pollinator networks. *Am Nat* 193(6):E149–E167
- United States Department of Agriculture Agricultural Research Service (2019) <https://www.ars.usda.gov/oc/br/ccd/index/>
- United States Environmental Protection Agency, Schedule for Review of Neonicotinoid Pesticides (2019) <https://www.epa.gov/pollinator-protection/schedule-review-neonicotinoid-pesticides>
- vanEngelsdorp D, Evans JD, Saegerman C et al (2009) Colony collapse disorder: a descriptive study. *PLoS ONE* 4(8):e6481
- Wikipedia (2019) [https://en.wikipedia.org/wiki/Colony\\_collapse\\_disorder](https://en.wikipedia.org/wiki/Colony_collapse_disorder)
- Willkinson D, Smith GC (2002) A model of the mite parasite, Varroa destructor, on honeybees (*Apis mellifera*) to investigate parameters important to mite population growth. *Ecol Model* 148:263–275

**Publisher's Note** Springer Nature remains neutral with regard to jurisdictional claims in published maps and institutional affiliations.